



Nonlinear vibration and dynamic instability analysis nanobeams under thermo-magneto-mechanical loads: a parametric excitation study

Farzad Ebrahimi¹ · S. Hamed S. Hosseini¹

Received: 3 May 2019 / Accepted: 20 July 2019 / Published online: 7 September 2019
© Springer-Verlag London Ltd., part of Springer Nature 2019

Abstract

The nonlinear vibration behavior and dynamic instability of Euler–Bernoulli nanobeams under thermo-magneto-mechanical loads is the main objective of the present paper. Firstly, a short Euler–Bernoulli nanobeam is modeled and exposed to an external parametric excitation. Based on the nonlocal continuum theory and nonlinear von Karman beam theory, the nonlinear governing differential equation of motion is derived. Secondly, to transport the partial differential equation to the ordinary differential equation, Galerkin method is applied. Then, multiple scales method, as an analytical approach, is used to solve the equation. At the end, modulation equation of Euler–Bernoulli nanobeams is obtained. Then, to evaluate the dynamic instability of the system, trivial and nontrivial steady-state solutions are discussed. Emphasizing the effect of parametric excitation, for considering the instability regions, bifurcation points are studied and investigated. As a result, it can be observed that the damping coefficient plays an effective role as well as parametric excitation in stability and frequency response of the system.

Keywords Nonlinear vibration · Parametric excitation · Dynamic instability · Thermo-magneto-mechanical load · Euler–Bernoulli nanobeam · Multiple scale

1 Introduction

It has been cleared that due to their attractive and distinctive electromechanical features, carbon nanostructures including carbon nanotube (CNT) and graphene sheet have attracted attention of many researchers and scholars who work and study in field of smart materials and engineering design. In fact, carbon nanotubes can be used in various kinds of electromechanical devices such as optical transparency [1, 2], resonators [3–5], diagnosis of gas atoms [6], memory devices [7] and composite material [8].

On the other hand, although it has been proved that the small-scale effects in nanostructures play a significant role in their characteristics and properties, classical plate theory (CLPT) is unable to evaluate and analyze the size effect in nanostructures [9]. Therefore, the nonlocal elasticity theory

developed by Eringen and Edelen [9, 10] has been widely accepted and applied to analyze the size effect of the nanostructures. In connection with use of the nonlocal elasticity theory, many theoretical studies [11–17] were conducted and developed by researchers. The investigations were continued by Mouffoki et al. [18] in considering vibration behavior of nanobeams using shear deformation beam theory. Bedia et al. [19] found that considering nonlocal parameter can have a significant role in buckling of nanobeams. Based on nonlocal elasticity theory, buckling of single layer graphene sheet (SLGS) was studied by Mokhtar et al. [20]. Nonlinear and mechanical behavior of nanobeams was investigated by other researches [21–23]. Kadari et al. [24] reported buckling analysis of nanoplate embedded on an elastic foundation. Using nonlocal strain gradient, Karami et al. [25–29] illustrated effect of considering nonlocal theories in mechanical analysis of nanostructures. In addition, mechanical behavior of functionally graded (FG) micro/nanobeams was considered by Ahouel et al. [30], Chaht et al. [31] and Tlidji et al. [32]. Furthermore, bending and vibration of composite plates were investigated by Abualnour et al. [33]. Using nonlocal elasticity theory, thermal buckling and vibration behavior of composite nanostructures including boron

✉ Farzad Ebrahimi
febrahimi@eng.ikiu.ac.ir

¹ Department of Mechanical Engineering, Faculty of Engineering, Imam Khomeini International University, Qazvin 3414896818, Iran

nitride nanotubes (BNNT) was conducted by Chikh et al. [34], Semmah [35] and Hamza-Cherif [36].

Currently, most researches on micro/nanobeam have focused on their nonlinear properties. It is worth mentioning that nonlinear or large amplitude vibration of beams, including nano and micro, exposed to very large displacements has an important place in engineering problems among literatures and investigations. In couple of the considerable works, Simsek [37, 38] investigated the nonlinear vibration of nanobeams based on nonlocal elasticity and strain gradient theories. The results showed the effect of small scale on the nonlinear frequency response. Nazemnezhad and Hosseini-Hashemi [39] presented nonlinear vibration of functionally graded (FG) nanobeams for different boundary conditions. It was found that unlike the linear vibration, the nonlinear vibration depends on the gradient index. Based on von Karman theory to analyze the effect of nonlinearity, the nonlinear frequency response of microbeams was conducted by Nourbakhsh et al. [40]. Oskouie et al. [41] presented nonlinear frequency response of viscoelastic Euler–Bernoulli nanobeams. They reported the viscoelasticity effect on nonlinear vibration behavior. Using multiple time scales method, nonlinear forced vibration of nanobeams subjected to moving concentrated load embedded on a viscoelastic foundation was conducted by Ghadiri et al. [42].

The concept of functionally gradient materials (FGMs) was first proposed by several Japanese materials researchers. Thanks to recent advances in FGM, numerous investigators have analyzed and developed FG plates [43–59]. Thermal analysis and considering thermal effect on FG plates is the main objective of these works. Results showed that thermal decreases vibrations of structures as well. Applying nonlocal shear deformation theory, Karami et al. [60], Besseghier et al. [61] and Bounouara et al. [62] demonstrated vibration and resonance characteristics of FG nanoplates. It was found that reinforcement patterns determine the resonance position. Also, in Ref. [57], a new shear strain shape function was developed and the results showed a good accuracy with other available results.

In the following, attention was given to porous materials. Using nonlocal theories including strain gradient theory, She et al. [63–66] analyzed mechanical behaviors including nonlinear bending and vibration and buckling in porous nanotubes and nanobeams. The results indicated that the characteristics of porous curved nanobeams are affected by small-scale parameter as well as geometry. Moreover, boundary conditions play a significant role in buckling behavior. In another work, She et al. [67] investigated wave propagation of porous nanotubes. Their results show that the deflection of the tube increases as the porosity rises. The possible reason is that a higher value of porosity volume corresponds to lower stiffness for the tubes. Fourn et al. [68] considered wave propagation in FG plates. Also, effect of

thickness stretching was analyzed by Bouhadra et al. [69] for composite plates.

Looking at previous researches, it can be observed that although there are many researches and studies in linear and nonlinear of micro and nano beams, nonlinear vibration and dynamic instability of beams and nanobeams has been untouched in many aspects [70, 71]. Recently, Huang et al. [72] studied dynamic instability of nanobeams exposed to parametric excitation. It was found that nonlocal parameter can affect the instability regions. In another work, parametric excitation of carbon nanotube was investigated by Wang et al. [73]. This study reported that external parametric excitation makes a gap between positive and negative bifurcation points. In fact, they move away from each other. Moreover, to analyze the effect of nonlocal parameter and axial force on the linear frequency and instability of nanobeams, the perturbation method was employed by Li et al. [74]. Bakhadda et al. [75] modeled a composite plate reinforced with carbon nanotube to analyze dynamic and bending. Employing nonlocal higher shear deformation theory, Bouadi et al. [76] presented an analysis for stability of single layer graphene sheet (SLGS). Besides, stability analysis of orthotropic SLGS was reported by Yazid et al. [77]. Considering surface effect, Youcef et al. [78] studied dynamic analysis of nanobeams. In another study, using first shear deformation theory, static and dynamic characteristics of sandwich plates were conducted by Draoui et al. [79].

More recently, because of the importance of parametric excitation on electromechanical systems and devices, the effect of parametric excitation on energy harvesting systems has been investigated [80–82]. In these researches, a Duffing oscillator has been used to model the behavior of energy harvesters. Besides, to study nonlinear vibration and stability of tapered-composite plate, a parametric excitation was employed [83]. Also, the effect of the van der Waals interaction on instability of double-walled nanobeams under a parametric excitation was analyzed by Wang [84]. Using Mathieu and Hill's equations, Krylov et al. [85] also presented pull-in instability of micro-devices under a parametric excitation. Lima and Sampaio [86] reported behavior of two parametric excited nonlinear systems. Hence, literature survey can indicate that the effects of both external parametric excitation and thermo-magneto-mechanical loads on nonlinear vibration and dynamic instability of nanobeams have not been studied in literatures.

This paper, for the first time, comprehensively studies the nonlinear frequency response and dynamic instability of nanobeams under thermo-magneto-mechanical loads, while it is subjected to an external parametric excitation. In the first step, a short nanobeam is modeled and an external axial force is applied to make the parametric excitation. Secondly, based on the nonlocal continuum theory and nonlinear von Karman beam theory, the nonlinear governing differential

equation of motion is derived. Then, Galerkin technique and multiple time scales approach are used to solve the equation. At the end, modulation equation and the dynamic instability of the nanobeam are derived. Finally, trivial and nontrivial steady-state solutions are discussed.

2 Problem formulation

Figure 1 shows the schematic of nanobeam embedded on a viscoelastic foundation under an axial force with length L , which is along the x -axis, and diameter d . The axial force is a function with a harmonic excitation with frequency Ω . In addition, deformation of the nanobeam is denoted by w , along the z -axis.

2.1 Constitutive relations

According to the nonlocal elasticity theory that was presented by Eringen [9, 10, 87, 88], the stress at a reference point X is considered to be a function of the strain field at every point X' in the body. The nonlocal stress tensor σ at point X can be defined as below:

$$\sigma = \int_V K(|X' - X|, \tau) \sigma'(X') dX', \tag{1}$$

where σ' is the classical stress tensor and $K(|X' - X|)$ is the Kernel function represents the nonlocal modulus. Eringen [10, 88] demonstrated that it is possible to represent the integral constitutive relation in an equivalent differential form as:

$$(1 - (e_0 a)^2 \nabla^2) \sigma = \sigma', \tag{2}$$

where $\nabla^2 = \frac{\partial^2}{\partial x^2} + \frac{\partial^2}{\partial y^2}$ the Laplacian operator and $(e_0 a)$ introduces the nonlocal parameter. In which, e_0 and a are a constant which is convenient to each material and an internal characteristic length, respectively. The value of e_0 needs to be determined from experiments or by matching the dispersion relation of plane waves with those of atomic lattice dynamics. Then, the nonlocal constitutive relation for the nanobeam is written as

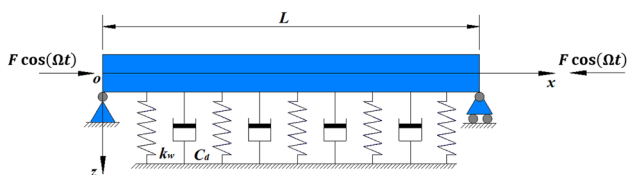


Fig. 1 The schematic of nanobeam embedded on a viscoelastic foundation under an axial force

$$\sigma_{xx} - (e_0 a)^2 \frac{\partial^2 \sigma_{xx}}{\partial x^2} = E \varepsilon_{xx} \tag{3}$$

In which, σ_{xx} , ε_{xx} are the axial normal stress and strain, respectively. Also, E indicates the Young’s modulus. Based on the Euler–Bernoulli beam model, the axial force and the resultant bending moment can be expressed as

$$\{N, M\} = \int_A \sigma_x(1, z) dA, \tag{4}$$

where z is the transverse coordinate in the deflection direction and A the area of the cross section of the nanobeam. Based on classical beam theory, the displacements can be written as below:

$$u_1(x, z, \tilde{t}) = u(x, \tilde{t}) - z \frac{\partial w}{\partial x}, \quad u_2 = 0, \quad u_3(x, z, \tilde{t}) = w(x, \tilde{t}) \tag{5}$$

In Eq. (5), u and w are the axial and transverse displacements of the nanobeam along x and z directions, respectively. Now, for the nonlinear von Karman strain, we can have:

$$\varepsilon = \varepsilon_0 + z \kappa, \tag{6}$$

where ε is the strain vector, and ε_0 and κ are the nonlinear strain vector and the variation of curvature vector, respectively, and can be defined as below:

$$\varepsilon_0 = \frac{\partial u_0}{\partial x} + \frac{1}{2} \left(\frac{\partial w}{\partial x} \right)^2, \quad \kappa = - \frac{\partial^2 w}{\partial x^2} \tag{7}$$

From Eqs. (3) to (7), the axial load and the bending moment can be obtained as following:

$$\begin{aligned} (1 - (e_0 a)^2 \nabla^2) N &= EA \varepsilon_0 \\ (1 - (e_0 a)^2 \nabla^2) M &= EI \kappa, \end{aligned} \tag{8}$$

where $I = \int_A z^2 dA$ is defined as the moment of inertia. Thus, the equation of motion can be written as [89, 90]:

$$\begin{aligned} EI \frac{\partial^4 w}{\partial x^4} - \frac{\partial}{\partial x} \left(N \frac{\partial w}{\partial x} \right) + (e_0 a)^2 \frac{\partial^3}{\partial x^3} \left(N \frac{\partial w}{\partial x} \right) \\ + \rho A \frac{\partial^2}{\partial \tilde{t}^2} \left[w - (e_0 a)^2 \frac{\partial^2 w}{\partial x^2} \right] = f - (e_0 a)^2 \frac{\partial^2 f}{\partial x^2} \end{aligned} \tag{9}$$

It can be obtained that the axial normal force N is as below:

$$N = \tilde{N}_x^{\text{mag}} + \tilde{N}_x^{\text{th}} + \tilde{N}_x^{\text{mec}} + F \cos \Omega \tilde{t} - \left[\frac{EA}{2L} \right] \int_0^L \left(\frac{\partial w}{\partial x} \right)^2 dx \tag{10}$$

In Eq. (10), \tilde{N}_x^{mag} , \tilde{N}_x^{th} , \tilde{N}_x^{mec} denote a uniaxial magnetic field, thermal load caused by temperature change and in-plane load caused by initial stress, respectively. The term of $(F \cos \Omega \tilde{t})$ is also the axial force that can cause a parametric excitation. We can define the parameters of the axial normal force as

$$\tilde{N}_x^{\text{mag}} = \eta H_x^2 \frac{\partial^2 w}{\partial x^2}, \quad \tilde{N}_x^{\text{th}} = \alpha EAT, \quad \tilde{N}_x^{\text{mec}} = \xi \sigma_0, \quad (11)$$

where H_x, η are in-plane uniaxial magnetic field and the magnetic field permeability, respectively. In fact, \tilde{N}_x^{mag} explains the Lorentz force along the x -axis [91]. In term of $\tilde{N}_x^{\text{th}}, \alpha, A$ and T demonstrate the coefficient of thermal expansion, the cross sectional area and the difference between the temperature gradient and its initial reference temperature, respectively. In addition, ξ and σ_0 are the compression ratio and the initial stress, respectively. For the present study, it is assumed that $\xi = 1$ and initial stress is along the x -axis direction. And also, in Eq. (9), f is defined as below:

$$f = k_w w + c_d \frac{\partial w}{\partial t}, \quad (12)$$

where k_w and c_d denote linear coefficient of Winkler and damper modulus parameter, respectively. The Winkler-type foundation can be modeled from Ref. [92]. At the end, to derive the equation of motion, we substitute Eqs. (10), (11) and (12) into Eq. (9) as

$$\begin{aligned} -EI \frac{\partial^4 w}{\partial x^4} - \left\{ \tilde{N}_x^{\text{mag}} + \tilde{N}_x^{\text{th}} + \tilde{N}_x^{\text{mec}} + F \cos \bar{\Omega} \tilde{t} - \left[\frac{EA}{2L} \right] \int_0^L \left(\frac{\partial w}{\partial x} \right)^2 dx \right\} \frac{\partial^2 w}{\partial x^2} + c_d \frac{\partial w}{\partial t} + k_w w \\ + (e_0 a)^2 \frac{\partial^4 w}{\partial x^4} \left\{ \tilde{N}_x^{\text{mag}} + \tilde{N}_x^{\text{th}} + \tilde{N}_x^{\text{mec}} + F \cos \bar{\Omega} \tilde{t} - \left[\frac{EA}{2L} \right] \int_0^L \left(\frac{\partial w}{\partial x} \right)^2 dx \right\} \\ - (e_0 a)^2 k_w \frac{\partial^2 w}{\partial x^2} - (e_0 a)^2 c_d \frac{\partial^3 w}{\partial \tilde{t} \partial x^2} = \rho A \left(\frac{\partial^2 w}{\partial \tilde{t}^2} - (e_0 a)^2 \frac{\partial^4 w}{\partial \tilde{t}^2 \partial x^2} \right) \end{aligned} \quad (13)$$

To have a good comparison between results, indirect parameters can be expressed as follows:

$$\begin{aligned} X = \frac{x}{L}, \quad W = \frac{w}{L}, \quad \gamma = \frac{e_0 a}{L}, \quad K_w = \frac{k_w L^4}{EI}, \quad N_x^{\text{th}} = \frac{\tilde{N}_x^{\text{th}} L^2}{EI}, \quad N_x^{\text{mag}} = \frac{\tilde{N}_x^{\text{mag}} L^2}{EI}, \\ N_x^{\text{mec}} = \frac{\tilde{N}_x^{\text{mec}} L^2}{EI}, \quad C_d = c_d \sqrt{\frac{L^4}{EI}}, \quad \Omega = \bar{\Omega} \sqrt{\frac{\rho A L^4}{EI}}, \quad t = \frac{\tilde{t}}{L^2} \sqrt{\frac{EI}{\rho A}}, \end{aligned} \quad (14)$$

Using these indirect parameters and substituting in the Eq (13), the governing equation of nanobeam will be obtained as follows:

$$\begin{aligned} -\frac{\partial^4 W}{\partial X^4} - \left\{ N_x^{\text{mag}} + N_x^{\text{th}} + N_x^{\text{mec}} + F \cos \Omega t - \int_0^L \left(\frac{\partial W}{\partial X} \right)^2 dX \right\} \frac{\partial^2 W}{\partial X^2} + C_d \frac{\partial W}{\partial t} + K_w W \\ + \gamma^2 \frac{\partial^4 W}{\partial X^4} \left\{ N_x^{\text{mag}} + N_x^{\text{th}} + N_x^{\text{mec}} + F \cos \Omega t - \int_0^L \left(\frac{\partial W}{\partial X} \right)^2 dX \right\} - \gamma^2 K_w \frac{\partial^2 W}{\partial X^2} \\ - \gamma^2 C_d \frac{\partial^3 W}{\partial t \partial X^2} = \left(\frac{\partial^2 W}{\partial t^2} - \gamma^2 \frac{\partial^4 W}{\partial t^2 \partial X^2} \right) \end{aligned} \quad (15)$$

The corresponding boundary conditions for simply supported nanobeam are defined as below:

$$W = 0, \quad \frac{\partial^2 W}{\partial X^2} = 0, \quad \text{at } X = 0, \quad X = L \quad (16)$$

2.2 Galerkin method

According to Galerkin method, to solve the governing equation of motion Eq. (15), an approximate solution, for simply supported boundary conditions, can be assumed as following,

$$W(x, t) = \psi(t) \sum_{n=1}^{\infty} \sin \frac{n\pi x}{L}. \quad (17)$$

Here, t is known as the time-dependent parameter and $\sin \frac{n\pi X}{L}$ is the spatial basis function, respectively. By substituting Eq. (17) into the Eq. (15) and for fundamental frequency ($n = 1$), the governing equation of motion yields:

$$\ddot{\psi} + \omega_0^2 \psi + 2\epsilon \mu \dot{\psi} + \epsilon \beta \psi^3 + \epsilon \delta \cos(\Omega t) \psi = 0, \quad (18)$$

where ϵ is scaling and a very small parameter $\epsilon (\ll 1)$ and other parameters are defined as below:

$$\begin{aligned} \omega_0^2 = \frac{1}{2} \left\{ K_w - (N_x^{\text{mag}} + N_x^{\text{th}} + N_x^{\text{mec}}) \right\} + \frac{1}{\left(1 + \gamma^2 \left(\frac{\pi}{L} \right)^2 \right)} \left(\frac{\pi}{L} \right)^4, \\ \beta = \frac{1}{4} \left(\frac{\pi}{L} \right)^4, \quad \mu = \frac{C_d}{2}, \quad \delta = -F \left(\frac{\pi}{L} \right)^2 \end{aligned} \quad (19)$$

2.3 Multiple time scales method

Multiple time scales as a practical method of perturbation procedures that, for the first time, was presented by Nayfeh and Mook [93] is applied to solve Eq. (18). To have the solutions for Eq. (18), at first, we assume $\Omega = 2\omega_0$ and then utilize a set of first-order approximations as:

$$\psi(t) = \psi_0(T_0, T_1) + \epsilon\psi_1(T_0, T_1) \tag{20}$$

Equation (20) is perturbation parameter which uses time scales (T_0, T_1) to determine the solution. Now, to determine the modulation of the amplitude and phase, it would be enough to use two time scales as follows:

$$T_0 = t, \quad T_1 = \epsilon t \tag{21}$$

Now, T_0 and T_1 define the fast and slow time scales, respectively. It is noted that T_1 is introduced as the nonlinear part of the set of approximation. According to Eq. (21), it can be defined as:

$$\frac{d}{dT} = \frac{d}{dT_0} + \epsilon \frac{d}{dT_1} + \dots = D_0 + D_1 + \dots \tag{22a}$$

$$\frac{d^2}{dT^2} = \frac{d^2}{dT_0^2} + 2\epsilon \frac{d}{dT_0} \frac{d}{dT_1} + \dots = D_0^2 + 2\epsilon D_0 D_1 + \dots \tag{22b}$$

At first, Eq. (20) and Eqs. (22a) (22b) are substituted in Eq. (18). Then, the coefficients of ϵ^0 and ϵ^1 are equated with zero; thus, we have:

$$\epsilon^0 : D_0^2 \psi_0 + \omega_0^2 \psi_0 = 0 \tag{23a}$$

$$\epsilon^1 : D_0^2 \psi_1 + \omega_0^2 \psi_1 = -2D_0 D_1 \psi_0 - 2\mu D_0 \psi_0 - \beta \psi_0^3 - \delta \psi_0 \cos \Omega T_0 \tag{23b}$$

To solve Eq. (23a), a general solution may be introduced as:

$$\psi_0 = A(T_1)e^{i\omega_0 T_0} + CC \tag{24}$$

Now, A is an unknown and CC is the complex conjugate of the other terms of the equation. Using the Eq. (24) and substituting in Eq. (23b), we can derive:

$$\begin{aligned} D_0^2 \psi_1 + \omega_0^2 \psi_1 = & -2i\omega_0 A' e^{i\omega_0 T_0} - 2i\mu\omega_0 A e^{i\omega_0 T_0} \\ & - \beta A^3 e^{3i\omega_0 T_0} - 3\beta A^2 \bar{A} e^{i\omega_0 T_0} \\ & - \frac{1}{2} \delta A (e^{i\Omega T_0} + e^{-i\Omega T_0}) e^{i\omega_0 T_0} + CC. \end{aligned} \tag{25}$$

Here, \bar{A} is the complex conjugate of A and CC denotes the complex conjugate of the other terms of the equation (including \bar{A}). Now, by definition ($\Omega = 2\Omega + \sigma\epsilon$) that σ is detuning parameter, we eliminate the secular terms in Eq. (25).

$$2i\omega_0(A' + \mu A) + 3\beta A^2 \bar{A} - \frac{1}{2} \delta \bar{A} e^{i\sigma T_1} = 0. \tag{26}$$

We need to define a polar form for A as below:

$$A = \frac{1}{2} a e^{i\lambda} = \frac{1}{2} a (\cos \lambda + i \sin \lambda) \tag{27}$$

In Eq. (27), the phase angle and the real part of the amplitude are shown by λ and a , respectively. Substituting the Eq. (27) into Eq. (26) and separating the real and imaginary parts, it can be derived as below:

$$a' = -\mu a + \frac{\delta}{4\omega_0} a \sin(\sigma T_1 - 2\lambda) \tag{28a}$$

$$a\lambda' = \frac{3}{8\omega_0} \beta a^3 - \frac{\delta}{4\omega_0} a \cos(\sigma T_1 - 2\lambda) \tag{28b}$$

To determine the steady-state response, we first transform Eq. (28), from a non-autonomous system to an autonomous one by defining $\eta = (\sigma T_1 - 2\lambda)$ and $\eta' = (\sigma - 2\lambda')$; then, Eqs. (28a) and (28b) are explained as follows:

$$a' = -\mu a + \frac{\delta}{4\omega_0} a \sin(\eta) \tag{29a}$$

$$a\eta' = \sigma a - \frac{3}{4\omega_0} \beta a^3 + \frac{\delta}{2\omega_0} a \cos(\eta) \tag{29b}$$

As a result, the steady-state response can be found by assuming: $a' = 0$ and $a\eta' = 0$; thus, modulation equations for the principal parametric resonance are expressed as:

$$-\mu a + \frac{\delta}{4\omega_0} a \sin(\eta) = 0 \tag{30a}$$

$$\sigma a - \frac{3}{4\omega_0} \beta a^3 + \frac{\delta}{2\omega_0} a \cos(\eta) = 0 \tag{30b}$$

2.4 Trivial steady-state response

Now, we are supposed to consider stability of the system. Firstly, defining Cartesian form of the solution ($A = \frac{1}{2}(p - iq)e^{i\lambda T_1}$), substituting A in Eq. (26), we rewrite the process of the solution as below:

$$\begin{aligned} i\omega_0(p' - iq') - \omega_0\lambda(p - iq) + i\mu\omega_0(p - iq) \\ + \frac{3\beta}{8}(p^2 - q^2 - 2ipq)(p + iq) + \frac{\delta}{4}(p + iq) = 0 \end{aligned} \tag{31}$$

In Eq. (31), the parameters of p and q are the function of T_1 . Now, at the same time, in order to make the equation autonomous, we need to have ($\lambda = \frac{\sigma}{2}$). In fact, for making the system autonomous, we need to consider the phase angle based on detuning parameter. Substituting ($\lambda = \frac{\sigma}{2}$) then, we can write:

$$\begin{cases} p' = -\frac{\sigma}{2}q - \mu p + \frac{3\beta}{8\omega_0}q(p^2 + q^2) - \frac{\delta}{4\omega_0}q \\ q' = \frac{\sigma}{2}p - \mu q - \frac{3\beta}{8\omega_0}p(p^2 + q^2) - \frac{\delta}{4\omega_0}p \end{cases} \quad (32)$$

Now, to analyze the stability of the system for trivial steady-state response, we should assume and substitute ($p = q = 0$). Thus, we form Jacobian matrix of the set of Eq. (32), as below:

$$A = \begin{bmatrix} -\mu & -\frac{\sigma}{2} - \frac{\delta}{4\omega_0} \\ \frac{\sigma}{2} - \frac{\delta}{4\omega_0} & -\mu \end{bmatrix} \quad (33)$$

Therefore, we can have determinant and trace of matrix A , as following:

$$\begin{cases} \Delta = \mu^2 + \left(\frac{\sigma^2}{4} - \frac{\delta^2}{16\omega_0^2}\right) \\ \tau = -2\mu \end{cases} \quad (34)$$

Finally, assuming ($\mu > 0$) and ($k = \frac{\delta}{2\omega_0}$), we are able to evaluate the stability of the system.

2.5 Non-trivial steady-state response

For a non-trivial solution of the system, the determinant of the coefficient matrix must vanish. To consider non-trivial steady-state response of the system, we have ($a \neq 0$). Thus, we will have:

$$\begin{cases} a' = 0 \Rightarrow -\mu a = -\frac{\delta a}{4\omega_0} \sin \eta \\ \eta' = 0 \Rightarrow \frac{1}{2}\sigma a = \frac{3\beta}{8\omega_0}a^3 + \frac{\delta a}{4\omega_0} \cos \eta \end{cases} \quad (35)$$

Applying trigonometric function ($\sin^2 \eta + \cos^2 \eta = 1$) in Eq. (35), we will have:

$$\mu^2 + \left(\frac{1}{2}\sigma - \frac{3\beta}{8\omega_0}a^2\right)^2 = \frac{\delta^2}{16\omega_0^2} \quad (36)$$

Finally, the amplitude a is obtained as:

$$a = \left[\frac{4\omega_0}{3\beta} \left(\sigma \pm \sqrt{\frac{\delta^2}{4\omega_0^2} - 4\mu^2} \right) \right]^{\frac{1}{2}} \quad (37)$$

It should be noted that the stability of the fixed points and the steady-state solution depends on the real part of the roots. If the real part of each root is positive, then the corresponding steady-state solution is unstable. And also, if the real part of each root is zero or negative, then the corresponding steady-state solution is stable.

3 Results and discussion

In this part, the results of the present work are discussed in details. However, before that, the accuracy of the numerical results has to be validated. Therefore, firstly, the numerical results are compared with other literatures in which their relations and results can be used to consider the accuracy of our numerical results. However, some effects such as thermo-magneto-mechanical exciting loads should be ignored.

3.1 Validation of the study

Firstly, to verify the accuracy of the formulation, Table 1 is presented. The numerical results of the present study reported in the table are compared with other available researches and literatures [39, 94, 95] so that, they are partly similar and close to our researches. Table 1 shows the nonlinear frequency ratio (ω_{NL}/ω_L) for amplitude–radius (w_{max}/r) ratio of isotropic beam with simply supported boundary conditions. The nonlinear frequency ratio is tabled for different amplitudes ratio [1–3]. Due to using a similar analytical approach, the results presented in Ref. [39] show more accuracy to the numerical results of the present work.

In Fig. 2, the relation between nonlinear frequency responses (σ) with respect to amplitude response (a) of a simply supported Euler–Bernoulli nanobeam compared with the results reported by Nourbakhsh et al. [40] is demonstrated. The nanobeam is subjected to an external excitation amplitude ($\delta = 0.1$). The results show a good agreement and precision. In this case, the damping coefficient (μ) and the nonlinear coefficient (β) are taken 0 and 100, respectively.

3.2 Numerical results and discussion

Now, numerical results, caused by applying both thermo-magneto-mechanical load and an external parametric excitation, are presented and discussed. In this section, emphasizing the effect of parametric excitation, for considering the instability regions, bifurcation points are studied and investigated. To clarify the concepts and make a better

Table 1 The frequency ratio (ω_{NL}/ω_L) at different maximum amplitude–radius (w_{max}/r) ratios of isotropic beam with simply supported boundary conditions

Amplitude ratio	Ref. [39]	Ref. [94]	Ref. [95]	Present work ratio
1	1.0937	1.0892	1.0897	1.0938
2	1.3750	1.3178	1.3229	1.3750
3	1.8438	1.6257	1.6394	1.8438

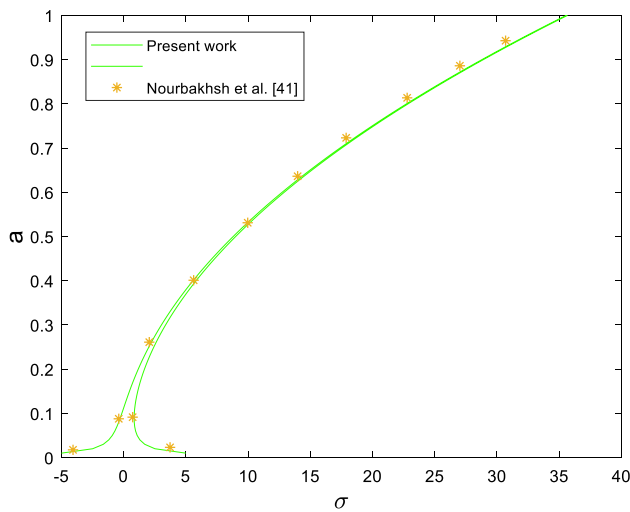


Fig. 2 The relation between nonlinear frequency responses (σ) with respect to amplitude response (a) of a simply supported Euler–Bernoulli nanobeam under an external excitation ($\delta = 0.1$) compared with the results reported by Nourbakhsh et al. [40] ($\mu = 0, \beta = 100$)

understanding, it is necessary to define some parameters in different regions of the graph.

The material properties of the system including nanobeam and elastic matrix are Young’s modulus $E = 1100$ Gpa, the mass density $\rho = 1.3$ g/cm³, the Winkler coefficient $k_w = 0.5$ Gpa and viscoelastic damping coefficient 3×10^{-7} Pa s. Besides, the nanobeam diameter is $d = 3$ nm and small-scale parameter is considered smaller than 2 nm [73].

Figure 3 shows the effect of detuning parameter (σ) with respect to the force amplitude of parametric excitation (k), as mentioned ($k = \frac{\delta}{2\omega_0}$), for linear ($\mu = 0$) and nonlinear ($\mu = 2$) states in different regions (I, II, III). The region (I) is always stable. There are two solutions in the region (II) including one trivial solution that is unstable and another nontrivial solution that is stable. In the region (III), there are three solutions including one trivial solution (stable) and two nontrivial solutions (stable and unstable). In Fig. 3, by changing the values of detuning parameter (σ) and force amplitude (k), we can observe different bifurcations.

The relation between the amplitude (a), force amplitude of the parametric excitation (k) and detuning parameter (σ) is presented in Fig. 4a, b. The point (σ_1) indicates a supercritical pitchfork bifurcation and the point (σ_2) represent a subcritical pitchfork in the beginning of region (III) that is unstable. In fact, before the point (σ_1), we have a trivial and stable solution and after that, in the region (II), we have a nontrivial and stable solution. Therefore, the state of the system changes in the point (σ_1) and also, in the point (σ_2). It should be noted that, to obtain these results, there are two

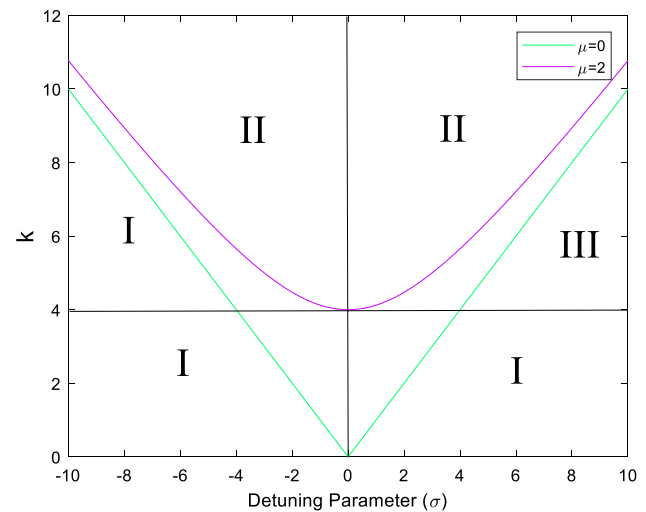


Fig. 3 The effect of detuning parameter (σ) with respect to the force amplitude of parametric excitation (k) for linear ($\mu = 0$) and nonlinear ($\mu = 2$) state in different regions of stability (I, II, III)

conditions, so that the force amplitude and nonlinearity must be ($k > 2\mu$) and ($\beta > 0$).

In fact, better to say, in Fig. 4a, detuning parameter (σ) is increased while the force amplitude is held constant. This process is represented by the line through points σ_1 and σ_2 . Before σ_1 , only the trivial solution exists, and it is stable. Between points σ_1 and σ_2 , the trivial solution is unstable, and the only realizable solution is given by Eq. (37). Beyond point σ_2 , the trivial solution is again stable and is the larger solution given by Eq. (37). Therefore, two solutions are realizable. From Fig. 4a, it can be inferred that in region II, all initial disturbances produce the same steady-state response (i.e., a limit cycle exists).

The effect of detuning parameter (σ) against the amplitude of parametric excitation (a) for different values of the force amplitude (k) can be observed in Fig. 5. As the force amplitude of the parametric excitation increases, amplitude (a) grows. Once again, different pitchfork bifurcations can be seen for different values of (k). Another point is that as the force amplitude increases, stable and unstable curves move far away from each other and make a gap between themselves.

The force amplitude of parametric excitation (k) versus the amplitude (a) for different values of the damping coefficient (μ) is shown in Fig. 6. In this plot, subcritical pitchfork bifurcations are shown. Besides, it can be observed that as damping coefficient changes, the bifurcation point situation shifts from one point to another. Dash lines denote non-trivial unstable solution in the region (III). As mentioned, the force amplitude (k) should be ($k > 2\mu$). The damping coefficient depends on parameter (C_d) of the foundation. In

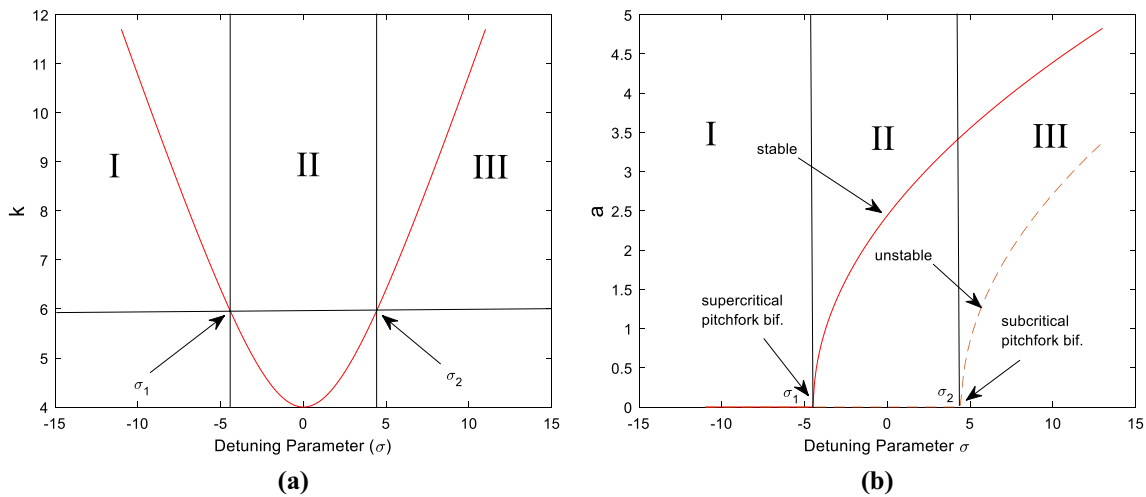


Fig. 4 **a** The effect of detuning parameter (σ) with respect to the force amplitude (k). **b** The effect of detuning parameter (σ) with respect to the amplitude of parametric excitation (a) for ($k = 6$)

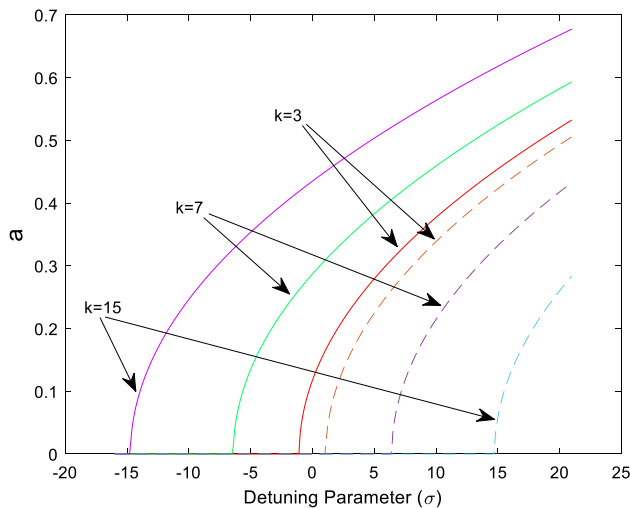


Fig. 5 The effect of detuning parameter (σ) against the amplitude of parametric excitation (a) for different values of the force amplitude (k)

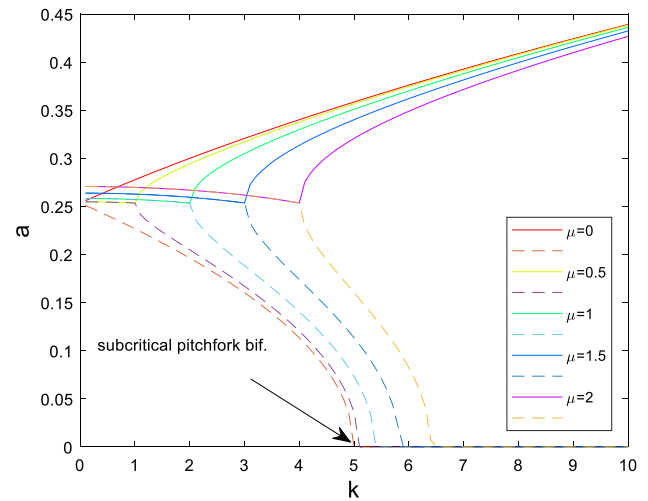


Fig. 6 The force amplitude of parametric excitation (k) versus the amplitude (a) for different values of the damping coefficient (μ)

Fig. 6, can trace the history of amplitude response as k is slowly increased from zero and then decreased.

Figure 7 shows the relation between the force amplitude of parametric excitation (k) versus the amplitude of the parametric excitation (a) for different values of temperatures (T) in regions (I), (II) and (III). As seen in Fig. 4, in negative detuning parameter ($\sigma < 0$) and positive detuning parameter ($\sigma > 0$), we will have different states. For ($\sigma = -5$), there is a supercritical pitchfork bifurcation between ($k = 5$) and ($k = 6$). However, as the detuning parameter becomes positive ($\sigma = 5$), bifurcation point transforms to a subcritical pitchfork bifurcation between regions (I) and (III). As seen in Fig. 4a, it means that the detuning parameter significantly

alters the stability of the system. Figures 8 and 9 can present the similar consequences. However, for uniaxial magnetic field values (Fig. 8) and initial stress values (Fig. 9), the amplitude of the system becomes completely different. Therefore, one of the results is that thermo-magneto-mechanical loads can only affect the amplitude of the system and are less important to determine the bifurcation point.

It is well known that the mechanical characteristics of nanostructures are size dependent. Thus, it is necessary to analyze the size effect on nonlinear vibration and dynamic instability of the system. The effect of nonlocal parameter (γ^2) is observed, while detuning parameter (σ) (Fig. 10) and the force amplitude (k) (Fig. 11) are constant.

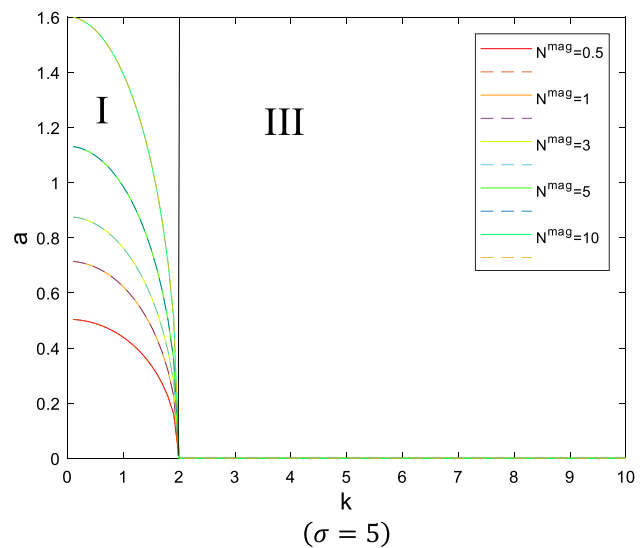
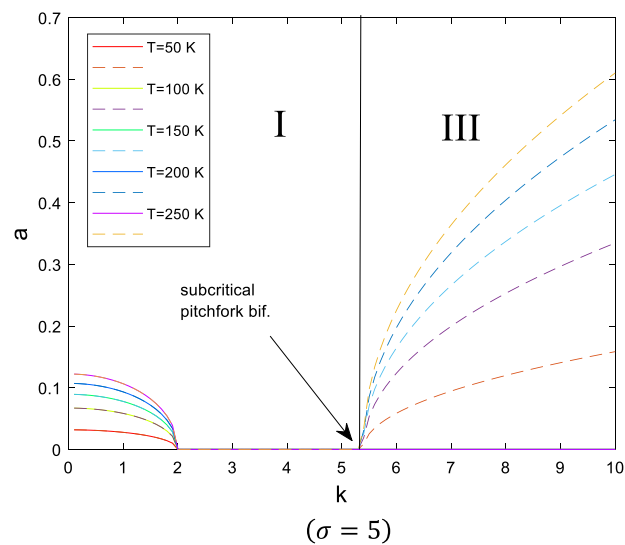
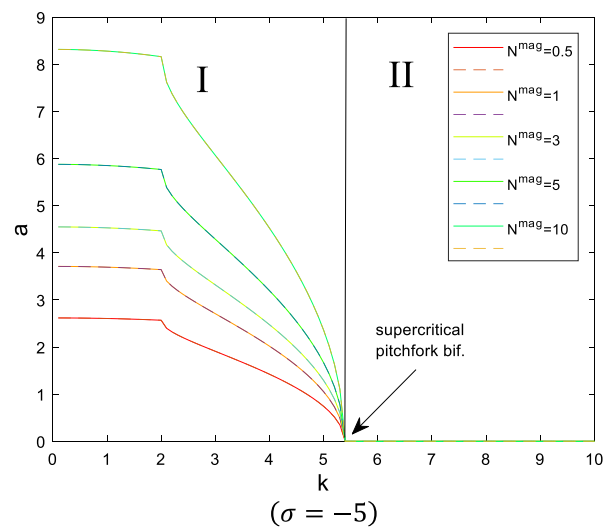
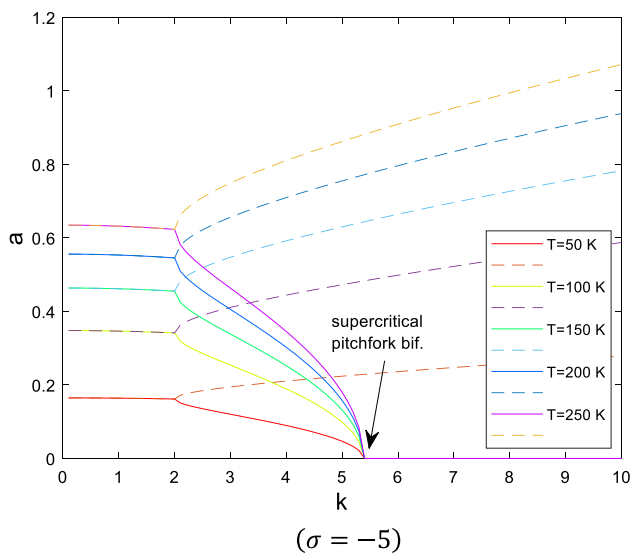


Fig. 7 The force amplitude of parametric excitation (k) versus the amplitude of the parametric excitation (a) for different values of temperatures (T) in regions (I), (II) and (III)

Fig. 8 The force amplitude of parametric excitation (k) versus the amplitude of the parametric excitation (a) for different values of uni-axial magnetic field (N^{mag}) in regions (I), (II) and (III)

In both figures, it can be inferred that as nonlocal parameter increases, the amplitude decays. In addition, nonlocal parameter is not effective on stability of the system and changes the bifurcation situation. Explanations made in Fig. 6 are valid and precise for Fig. 10. From Figs. 10 and 11 can be resulted that change in nonlocal parameter cannot change the stability of the system. It can only influence the amplitude of the system. Another point is that, in Fig. 10, we have a saddle node bifurcation in region (I). In Fig. 11, two pitchfork bifurcations including super and sub-critical bifurcations are seen.

Figure 12 indicates that unlike the other parameters such as nonlocal and thermo-magneto-mechanical loads, damping coefficient of the foundation plays an important role to

change the regions of stability of the system. It is observed that as damping coefficient increases, the bifurcation point shifts to higher detuning parameters, while it has a little effect on the amplitude (a).

The force amplitude of parametric excitation (k) with respect to the amplitude (a) for nondimensional Winkler coefficient (k_w) for detuning parameter ($\sigma = -3$) is shown in Fig. 13. As Winkler coefficient (k_w) increases, the amplitude grows. However, it has no effect on situation of bifurcation point. Figure 13 explains that by moving from the region (I) to the region (II), a pitchfork bifurcation occurs; however, the system is still stable.

Figure 14 states that the relation between the force amplitude of parametric excitation (k), the amplitude of the parametric excitation (a) and nonlinearity coefficients (β) for

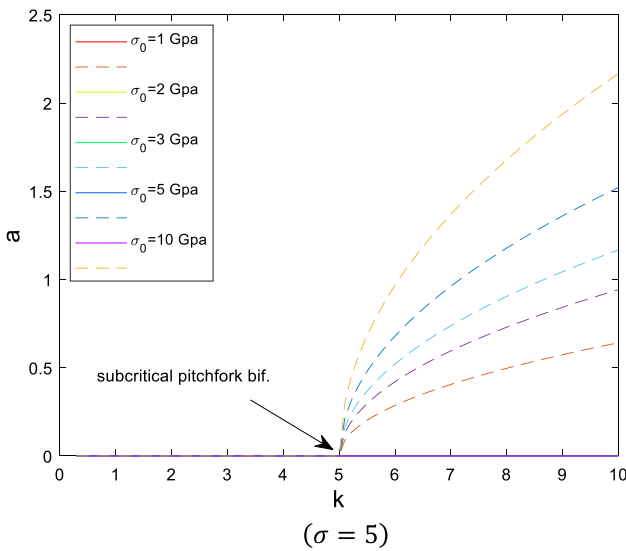
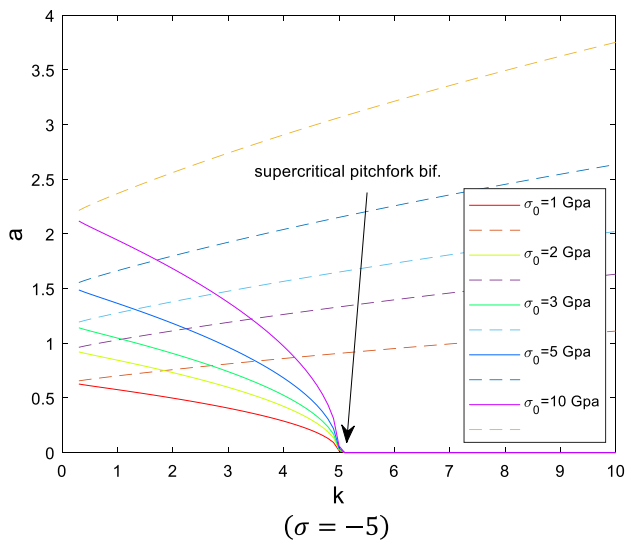


Fig. 9 The force amplitude of parametric excitation (k) versus the amplitude (a) for different values of initial stress (σ_0) in regions (I), (II) and (III)

detuning parameters ($\sigma = -5, 5$). Again, it is clear that non-linearity coefficient cannot change the stability of the system for both negative and positive detuning parameter. Moreover, it can strengthen the amplitude of the system. For ($\sigma = 5$), as seen, where the force amplitude of parametric excitation ($k = 2$), we have saddle node bifurcation that means a stable point and an unstable one collide to each other.

The numerical results of the present study should be regarded from different aspects. Firstly, considering Figs. 10 and 11, applying nonlocal elasticity theory can result in a more proper and accurate model. In addition, as can be observed in Figs. 7, 8 and 9, an increase or decrease in thermo-magneto-mechanical loads can result in instability of the system. For instance, in Fig. 7 ($\sigma = -5$), for various

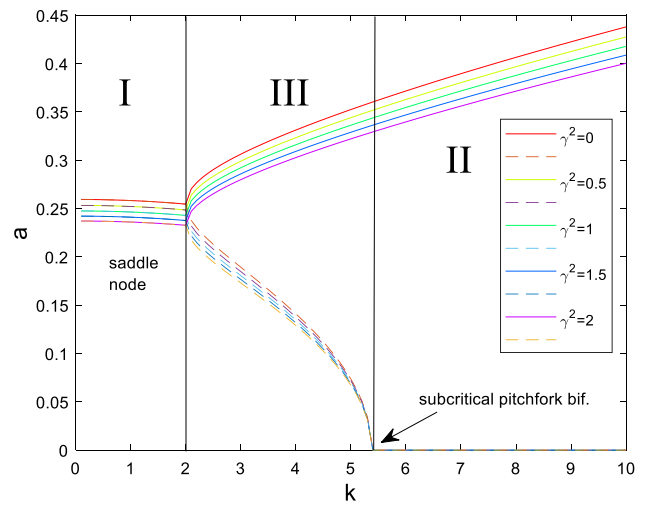


Fig. 10 The force amplitude of parametric excitation (k) against the amplitude of the parametric excitation (a) for different values of non-dimensional nonlocal parameter (γ^2) in regions (I, II) and (III)

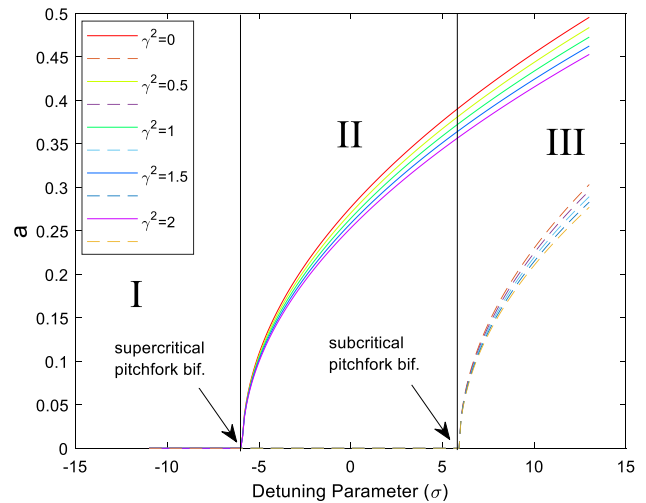


Fig. 11 The effect of detuning parameter (σ) with respect to amplitude of the parametric excitation (a) for different values of non-dimensional nonlocal parameter (γ^2) for ($k = 3$) in regions (I, II) and (III)

values of temperature, we have a distinct saddle point bifurcation which means a different stability region for the system. Observations made in Fig. 7 ($\sigma = -5$) are valid for Fig. 9 ($\sigma < 0$).

Secondly, it is clear that external loads such as thermo-magneto-mechanical loads will not be able to change the position of some special bifurcation points such as super and sub-critical pitchfork bifurcations. It means that the amplitude of external excitation has a little role in instability of the system compared to damping coefficient.

Another considerable result is the effect of external loads on amplitude response of the system. As seen in Figs. 7, 8 and 9, for both negative ($\sigma < 0$) and positive ($\sigma > 0$)

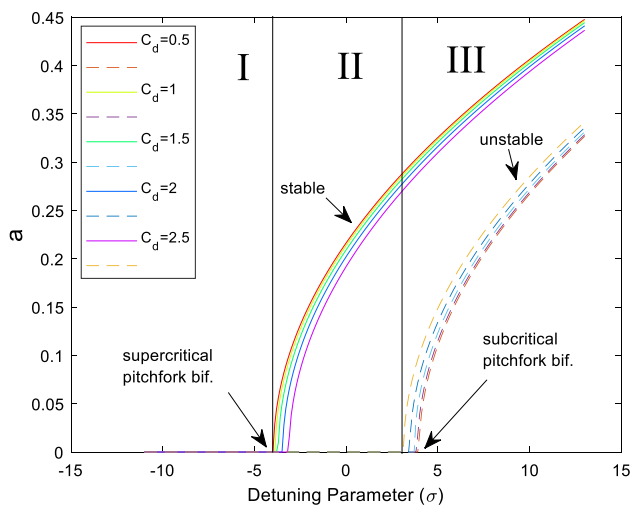


Fig. 12 The effect of detuning parameter (σ) with respect to amplitude of the parametric excitation (a) for different values of nondimensional damping coefficient (C_d) for ($k = 3$)

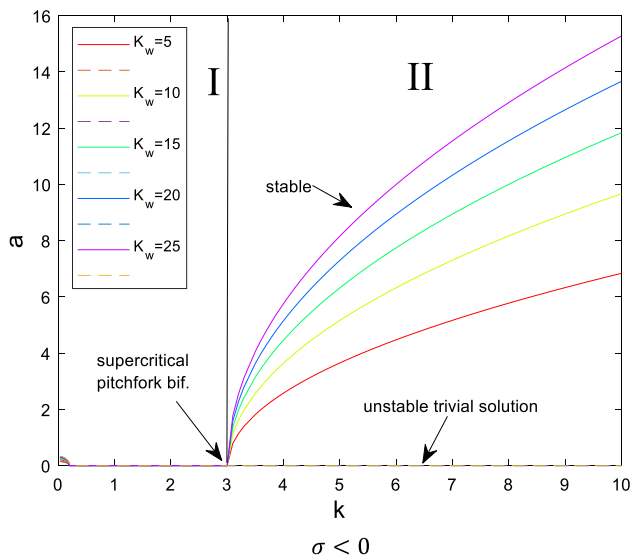


Fig. 13 The force amplitude of parametric excitation (k) versus the amplitude (a) for nondimensional Winkler coefficient (k_w) for detuning parameter ($\sigma = -3$)

situations, an increase in external loads leads to an increase in amplitude response. Whereas, as the amplitude of the motion grows, the nonlinear effects come into play and limit the growth. Therefore, the role of thermo-magneto-mechanical loads on dynamic instability of the system cannot be ignored. Another conclusion from results is that, for the linear as well as the nonlinear system, the phasing (including regions I, II and III) is such that the force actually does negative work and thus contributes to the decay.

4 Conclusions

The nonlinear vibration behavior and dynamic instability of nanobeams under thermo-magneto-mechanical load is the objective of present paper. Firstly, a short nanobeam is modeled such that it is embedded on a viscoelastic foundation and also subjected to an axial parametric force. Length of the nanobeam is L which is along the x -axis and diameter of the nanobeam is d . The axial force is a function with a harmonic excitation with frequency Ω and produces a parametric excitation. In addition, deformation of the nanobeam is denoted by w , along the z -axis. Based on the nonlocal elasticity theory and nonlinear von Karman deformation beam theory, the nonlinear governing equation of motion is derived. Secondly, to transport the partial differential equation to the ordinary differential equation, Galerkin technique is applied. Then, multiple time scales method, as an analytical approach, is used to solve the equation. At the end, modulation equation of nanobeams is obtained. Then, to evaluate the dynamic instability of the system, trivial and nontrivial steady-state solutions are discussed.

To evaluate the stability of the triple regions, emphasizing the effect of parametric excitation, bifurcation points including saddle node, supercritical pitchfork and subcritical pitchfork are studied and discussed. Therefore, it can be observed that the damping coefficient plays an effective role as well as parametric excitation in stability and frequency response of the system. In addition, thermo-magneto-mechanical loads make the amplitude response (a) grow or decay. The other main results of the study can be listed as below:

- The damping coefficient can affect the stability of the system while, other factors such as nonlocal parameter, Winkler coefficient are less important.
- The parametric excitation caused by external axial force plays a significant role in stability of the system.
- The stability of the system is significantly depends on whether detuning parameter is positive or negative.
- Amplitude response appears as a function of the frequency of the excitation.
- If the initial amplitude is very large, the response will decay until the steady-state solution is reached.
- As the force amplitude increases, stable and unstable curves move far away from each other and make a gap between themselves.
- Responses to all initial disturbances, regardless of how large the amplitude, decay in region I.

Besides, the results emphasize that considering nonlocal elasticity theory makes a proper and more accurate model to evaluate the effect of small scale and interaction between atoms. Also, numerical results can be utilized as benchmarks

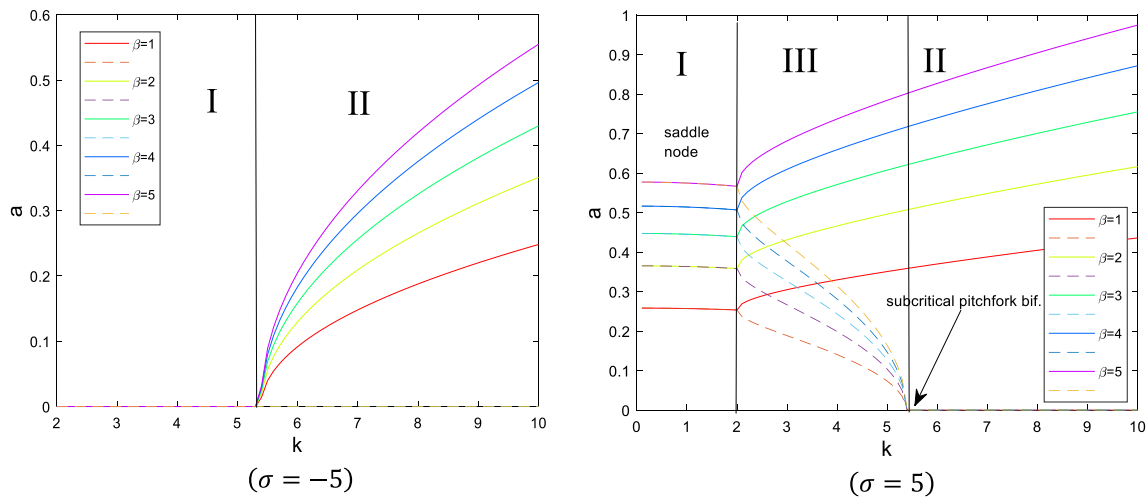


Fig. 14 The force amplitude of parametric excitation (k) versus the amplitude of the parametric excitation (a) for nonlinearity coefficients (β) for detuning parameters ($\sigma = -5, 5$)

for next analyses of nanobeams which are considered as one of the fundamental elements in nano-electromechanical systems.

References

- Eda G, Fanchini G, Chhowalla M (2008) Large-area ultrathin films of reduced graphene oxide as a transparent and flexible electronic material. *Nat Nanotechnol* 3(5):270
- Li D, Müller MB, Gilje S, Kaner RB, Wallace GG (2008) Processable aqueous dispersions of graphene nanosheets. *Nat Nanotechnol* 3(2):101
- Potekin R, Kim S, McFarland DM, Bergman LA, Cho H, Vakakis AF (2018) A micromechanical mass sensing method based on amplitude tracking within an ultra-wide broadband resonance. *Nonlinear Dyn* 92(2):287–304
- Mahmoud MA (2016) Validity and accuracy of resonance shift prediction formulas for microcantilevers: a review and comparative study. *Crit Rev Solid State Mater Sci* 41(5):386–429
- Ji Y, Choe M, Cho B, Song S, Yoon J, Ko HC, Lee T (2012) Organic nonvolatile memory devices with charge trapping multilayer graphene film. *Nanotechnology* 23(10):105202
- Arash B, Wang Q (2013) Detection of gas atoms with carbon nanotubes. *Sci Rep* 3:1782
- Bunch JS, Van Der Zande AM, Verbridge SS, Frank IW, Tanenbaum DM, Parpia JM, McEuen PL (2007) Electromechanical resonators from graphene sheets. *Science* 315(5811):490–493
- Kuilla T, Bhadra S, Yao D, Kim NH, Bose S, Lee JH (2010) Recent advances in graphene based polymer composites. *Prog Polym Sci* 35(11):1350–1375
- Eringen AC, Edelen DGB (1972) On nonlocal elasticity. *Int J Eng Sci* 10(3):233–248
- Eringen AC (1983) Theories of nonlocal plasticity. *Int J Eng Sci* 21(7):741–751
- Ghadiri M, Shafiei N, Akbarshahi A (2016) Influence of thermal and surface effects on vibration behavior of nonlocal rotating Timoshenko nanobeam. *Appl Phys A* 122(7):673
- Rahmanian S, Ghazavi MR, Hosseini-Hashemi S (2019) On the numerical investigation of size and surface effects on nonlinear dynamics of a nanoresonator under electrostatic actuation. *J Braz Soc Mech Sci Eng* 41(1):16
- Zhang YQ, Liu GR, Wang JS (2004) Small-scale effects on buckling of multiwalled carbon nanotubes under axial compression. *Phys Rev B* 70(20):205430
- Barretta R, Feo L, Luciano R, de Sciarra FM (2015) Variational formulations for functionally graded nonlocal Bernoulli–Euler nanobeams. *Compos Struct* 129:80–89
- Ghadiri M, Safi M (2017) Nonlinear vibration analysis of functionally graded nanobeam using homotopy perturbation method. *Adv Appl Math Mech* 9(1):144–156
- Ehyaeei J, Akbarshahi A, Shafiei N (2017) Influence of porosity and axial preload on vibration behavior of rotating FG nanobeam. *Adv Nano Res* 5(2):141–169
- Ebrahimi F, Hosseini SHS (2016) Thermal effects on nonlinear vibration behavior of viscoelastic nanosize plates. *J Therm Stresses* 39(5):606–625
- Mouffoki A, Bedia EA, Houari MSA, Tounsi A, Mahmoud SR (2017) Vibration analysis of nonlocal advanced nanobeams in hygro-thermal environment using a new two-unknown trigonometric shear deformation beam theory. *Smart Struct Syst* 20(3):369–383
- Bedia WA, Houari MSA, Bessaim A, Bousahla AA, Tounsi A, Saeed T, Alhodaly MS (2019) A new hyperbolic two-unknown beam model for bending and buckling analysis of a nonlocal strain gradient nanobeams. *J Nano Res* 57:175–191
- Mokhtar Y, Heireche H, Bousahla AA, Houari MSA, Tounsi A, Mahmoud SR (2018) A novel shear deformation theory for buckling analysis of single layer graphene sheet based on nonlocal elasticity theory. *Smart Struct Syst* 21(4):397–405
- Bellifa H, Benrahou KH, Bousahla AA, Tounsi A, Mahmoud SR (2017) A nonlocal zeroth-order shear deformation theory for nonlinear postbuckling of nanobeams. *Struct Eng Mech* 62(6):695–702
- Zemri A, Houari MSA, Bousahla AA, Tounsi A (2015) A mechanical response of functionally graded nanoscale beam: an assessment of a refined nonlocal shear deformation theory beam theory. *Struct Eng Mech* 54(4):693–710
- Bouafia K, Kaci A, Houari MSA, Benzair A, Tounsi A (2017) A nonlocal quasi-3D theory for bending and free flexural vibration behaviors of functionally graded nanobeams. *Smart Struct Syst* 19(2):115–126

24. Kadari B, Bessaim A, Tounsi A, Heireche H, Bousahla AA, Houari MSA (2018) Buckling analysis of orthotropic nanoscale plates resting on elastic foundations. *J Nano Res* 55:42–56
25. Karami B, Janghorban M, Tounsi A (2018) Variational approach for wave dispersion in anisotropic doubly-curved nanoshells based on a new nonlocal strain gradient higher order shell theory. *Thin Walled Struct* 129:251–264
26. Karami B, Janghorban M, Tounsi A (2018) Nonlocal strain gradient 3D elasticity theory for anisotropic spherical nanoparticles. *Steel Compos Struct* 27(2):201–216
27. Karami B, Janghorban M, Shahsavari D, Tounsi A (2018) A size-dependent quasi-3D model for wave dispersion analysis of FG nanoplates. *Steel Compos Struct* 28(1):99–110
28. Karami B, Janghorban M, Tounsi A (2017) Effects of triaxial magnetic field on the anisotropic nanoplates. *Steel Compos Struct* 25(3):361–374
29. Karami B, Shahsavari D, Nazemosadat SMR, Li L, Ebrahimi A (2018) Thermal buckling of smart porous functionally graded nanobeam rested on Kerr foundation. *Steel Compos Struct* 29(3):349–362
30. Ahouel M, Houari MSA, Bedia EA, Tounsi A (2016) Size-dependent mechanical behavior of functionally graded trigonometric shear deformable nanobeams including neutral surface position concept. *Steel Compos Struct* 20(5):963–981
31. Chaht FL, Kaci A, Houari MSA, Tounsi A, Bég OA, Mahmoud SR (2015) Bending and buckling analyses of functionally graded material (FGM) size-dependent nanoscale beams including the thickness stretching effect. *Steel Compos Struct* 18(2):425–442
32. Tlidji Y, Zidour M, Draiche K, Safa A, Bourada M, Tounsi A, Mahmoud SR (2019) Vibration analysis of different material distributions of functionally graded microbeam. *Struct Eng Mech* 69(6):637–649
33. Abualnour M, Houari MSA, Tounsi A, Mahmoud SR (2018) A novel quasi-3D trigonometric plate theory for free vibration analysis of advanced composite plates. *Compos Struct* 184:688–697
34. Chikh A, Tounsi A, Hebali H, Mahmoud SR (2017) Thermal buckling analysis of cross-ply laminated plates using a simplified HSDT. *Smart Struct Syst* 19(3):289–297
35. Semmah A, Heireche H, Bousahla AA, Tounsi A (2019) Thermal buckling analysis of SWBNNT on Winkler foundation by nonlocal FSDT. *Adv Nano Res* 7(2):89–98
36. Hamza-Cherif R, Meradjah M, Zidour M, Tounsi A, Belmahi S, Bensattalah T (2018) Vibration analysis of nano beam using differential transform method including thermal effect. *J Nano Res* 54:1–14
37. Şimşek M (2014) Large amplitude free vibration of nanobeams with various boundary conditions based on the nonlocal elasticity theory. *Compos B Eng* 56:621–628
38. Şimşek M (2016) Nonlinear free vibration of a functionally graded nanobeam using nonlocal strain gradient theory and a novel Hamiltonian approach. *Int J Eng Sci* 105:12–27
39. Nazemzhad R, Hosseini-Hashemi S (2014) Nonlocal nonlinear free vibration of functionally graded nanobeams. *Compos Struct* 110:192–199
40. Nourbakhsh H, Mohammadzadeh R, Rafiee M, Rafiee R (2012) Nonlinear effects on resonance behaviour of beams in micro scale. *Appl Mech Mater* 110:4178–4186
41. Oskouie MF, Ansari R, Sadeghi F (2017) Nonlinear vibration analysis of fractional viscoelastic Euler–Bernoulli nanobeams based on the surface stress theory. *Acta Mech Solida Sin* 30(4):416–424
42. Ghadiri M, Rajabpour A, Akbarshahi A (2017) Non-linear forced vibration analysis of nanobeams subjected to moving concentrated load resting on a viscoelastic foundation considering thermal and surface effects. *Appl Math Model* 50:676–694
43. Attia A, Bousahla AA, Tounsi A, Mahmoud SR, Alwabri AS (2018) A refined four variable plate theory for thermoelastic analysis of FGM plates resting on variable elastic foundations. *Struct Eng Mech* 65(4):453–464
44. Menasria A, Bouhadra A, Tounsi A, Bousahla AA, Mahmoud SR (2017) A new and simple HSDT for thermal stability analysis of FG sandwich plates. *Steel Compos Struct* 25(2):157–175
45. El-Haina F, Bakora A, Bousahla AA, Tounsi A, Mahmoud SR (2017) A simple analytical approach for thermal buckling of thick functionally graded sandwich plates. *Struct Eng Mech* 63(5):585–595
46. Bousahla AA, Benyoucef S, Tounsi A, Mahmoud SR (2016) On thermal stability of plates with functionally graded coefficient of thermal expansion. *Struct Eng Mech* 60(2):313–335
47. Boudierba B, Houari MSA, Tounsi A, Mahmoud SR (2016) Thermal stability of functionally graded sandwich plates using a simple shear deformation theory. *Struct Eng Mech* 58(3):397–422
48. Khetir H, Bouiadjra MB, Houari MSA, Tounsi A, Mahmoud SR (2017) A new nonlocal trigonometric shear deformation theory for thermal buckling analysis of embedded nanosize FG plates. *Struct Eng Mech* 64(4):391–402
49. Fahsi A, Tounsi A, Hebali H, Chikh A, Adda Bedia EA, Mahmoud SR (2017) A four variable refined nth-order shear deformation theory for mechanical and thermal buckling analysis of functionally graded plates. *Geomech Eng* 13(3):385–410
50. Beldjelili Y, Tounsi A, Mahmoud SR (2016) Hygro-thermo-mechanical bending of S-FGM plates resting on variable elastic foundations using a four-variable trigonometric plate theory. *Smart Struct Syst* 18(4):755–786
51. Hamidi A, Houari MSA, Mahmoud SR, Tounsi A (2015) A sinusoidal plate theory with 5-unknowns and stretching effect for thermomechanical bending of functionally graded sandwich plates. *Steel Compos Struct* 18(1):235–253
52. Belkorissat I, Houari MSA, Tounsi A, Bedia EA, Mahmoud SR (2015) On vibration properties of functionally graded nano-plate using a new nonlocal refined four variable model. *Steel Compos Struct* 18(4):1063–1081
53. Bourada F, Bousahla AA, Bourada M, Azzaz A, Zinata A, Tounsi A (2019) Dynamic investigation of porous functionally graded beam using a sinusoidal shear deformation theory. *Wind Struct* 28(1):19–30
54. Abdelaziz HH, Meziane MAA, Bousahla AA, Tounsi A, Mahmoud SR, Alwabri AS (2017) An efficient hyperbolic shear deformation theory for bending, buckling and free vibration of FGM sandwich plates with various boundary conditions. *Steel Compos Struct* 25(6):693–704
55. Meksi R, Benyoucef S, Mahmoudi A, Tounsi A, Adda Bedia EA, Mahmoud SR (2019) An analytical solution for bending, buckling and vibration responses of FGM sandwich plates. *J Sandw Struct Mater* 21(2):727–757
56. Younsi A, Tounsi A, Zaoui FZ, Bousahla AA, Mahmoud SR (2018) Novel quasi-3D and 2D shear deformation theories for bending and free vibration analysis of FGM plates. *Geomech Eng* 14(6):519–532
57. Zaoui FZ, Ouinas D, Tounsi A (2019) New 2D and quasi-3D shear deformation theories for free vibration of functionally graded plates on elastic foundations. *Compos B Eng* 159:231–247
58. Belabed Z, Bousahla AA, Houari MSA, Tounsi A, Mahmoud SR (2018) A new 3-unknown hyperbolic shear deformation theory for vibration of functionally graded sandwich plate. *Earthq Struct* 14(2):103–115
59. Houari MSA, Tounsi A, Bessaim A, Mahmoud SR (2016) A new simple three-unknown sinusoidal shear deformation theory for functionally graded plates. *Steel Compos Struct* 22(2):257–276
60. Karami B, Shahsavari D, Janghorban M, Tounsi A (2019) Resonance behavior of functionally graded polymer composite

- nanoplates reinforced with graphene nanoplatelets. *Int J Mech Sci* 156:94–105
61. Besseghier A, Houari MSA, Tounsi A, Mahmoud SR (2017) Free vibration analysis of embedded nanosize FG plates using a new nonlocal trigonometric shear deformation theory. *Smart Struct Syst* 19(6):601–614
 62. Bounouara F, Benrahou KH, Belkorissat I, Tounsi A (2016) A nonlocal zeroth-order shear deformation theory for free vibration of functionally graded nanoscale plates resting on elastic foundation. *Steel Compos Struct* 20(2):227–249
 63. She GL, Yuan FG, Ren YR, Xiao WS (2017) On buckling and postbuckling behavior of nanotubes. *Int J Eng Sci* 121:130–142
 64. She GL, Yuan FG, Ren YR, Liu HB, Xiao WS (2018) Nonlinear bending and vibration analysis of functionally graded porous tubes via a nonlocal strain gradient theory. *Compos Struct* 203:614–623
 65. She GL, Ren YR, Yuan FG, Xiao WS (2018) On vibrations of porous nanotubes. *Int J Eng Sci* 125:23–35
 66. She GL, Ren YR, Yan KM (2019) On snap-buckling of porous FG curved nanobeams. *Acta Astronaut* 161:475–484
 67. She GL, Yuan FG, Ren YR (2018) On wave propagation of porous nanotubes. *Int J Eng Sci* 130:62–74
 68. Fourn H, Atmane HA, Bourada M, Bousahla AA, Tounsi A, Mahmoud SR (2018) A novel four variable refined plate theory for wave propagation in functionally graded material plates. *Steel Compos Struct* 27(1):109–122
 69. Bouhadra A, Tounsi A, Bousahla AA, Benyoucef S, Mahmoud SR (2018) Improved HSDT accounting for effect of thickness stretching in advanced composite plates. *Struct Eng Mech* 66(1):61–73
 70. de Oliveira FM, Greco M (2015) Nonlinear dynamic analysis of beams with layered cross sections under moving masses. *J Braz Soc Mech Sci Eng* 37(2):451–462
 71. Arani AG, Abdollahian M, Kolahchi R (2015) Nonlinear vibration of a nanobeam elastically bonded with a piezoelectric nanobeam via strain gradient theory. *Int J Mech Sci* 100:32–40
 72. Huang Y, Fu J, Liu A (2018) Dynamic instability of Euler–Bernoulli nanobeams subject to parametric excitation. *Compos B Eng* 164:226–234
 73. Wang YZ, Wang YS, Ke LL (2016) Nonlinear vibration of carbon nanotube embedded in viscous elastic matrix under parametric excitation by nonlocal continuum theory. *Physica E* 83:195–200
 74. Li C, Lim CW, Yu JL (2010) Dynamics and stability of transverse vibrations of nonlocal nanobeams with a variable axial load. *Smart Mater Struct* 20(1):015023
 75. Bakhadda B, Bouiadjra MB, Bourada F, Bousahla AA, Tounsi A, Mahmoud SR (2018) Dynamic and bending analysis of carbon nanotube-reinforced composite plates with elastic foundation. *Wind Struct* 27(5):311–324
 76. Bouadi A, Bousahla AA, Houari MSA, Heireche H, Tounsi A (2018) A new nonlocal HSDT for analysis of stability of single layer graphene sheet. *Adv Nano Res* 6(2):147–162
 77. Yazid M, Heireche H, Tounsi A, Bousahla AA, Houari MSA (2018) A novel nonlocal refined plate theory for stability response of orthotropic single-layer graphene sheet resting on elastic medium. *Smart Struct Syst* 21(1):15–25
 78. Youcef DO, Kaci A, Benzair A, Bousahla AA, Tounsi A (2018) Dynamic analysis of nanoscale beams including surface stress effects. *Smart Struct Syst* 21(1):65–74
 79. Draoui A, Zidour M, Tounsi A, Adim B (2019) Static and dynamic behavior of nanotubes-reinforced sandwich plates using (FSDT). *J Nano Res* 57:117–135
 80. Alevras P, Theodossiades S, Rahnejat H (2017) Broadband energy harvesting from parametric vibrations of a class of nonlinear Mathieu systems. *Appl Phys Lett* 110(23):233901
 81. Amer YA, El-Sayed AT, Kotb AA (2016) Nonlinear vibration and of the Duffing oscillator to parametric excitation with time delay feedback. *Nonlinear Dyn* 85(4):2497–2505
 82. Bobryk RV, Yurchenko D (2016) On enhancement of vibration-based energy harvesting by a random parametric excitation. *J Sound Vib* 366:407–417
 83. Darabi M, Ganesan R (2017) Non-linear vibration and dynamic instability of internally-thickness-tapered composite plates under parametric excitation. *Compos Struct* 176:82–104
 84. Wang YZ (2017) Nonlinear internal resonance of double-walled nanobeams under parametric excitation by nonlocal continuum theory. *Appl Math Model* 48:621–634
 85. Krylov S, Harari I, Cohen Y (2005) Stabilization of electrostatically actuated microstructures using parametric excitation. *J Micromech Microeng* 15(6):1188
 86. Lima R, Sampaio R (2016) Two parametric excited nonlinear systems due to electromechanical coupling. *J Braz Soc Mech Sci Eng* 38(3):931–943
 87. Eringen AC (1972) Nonlocal polar elastic continua. *Int J Eng Sci* 10(1):1–16
 88. Eringen AC (1983) On differential equations of nonlocal elasticity and solutions of screw dislocation and surface waves. *J Appl Phys* 54(9):4703–4710
 89. Emam SA (2009) A static and dynamic analysis of the postbuckling of geometrically imperfect composite beams. *Compos Struct* 90(2):247–253
 90. Emam SA, Nayfeh AH (2009) Postbuckling and free vibrations of composite beams. *Compos Struct* 88(4):636–642
 91. Murmu T, McCarthy MA, Adhikari S (2013) In-plane magnetic field affected transverse vibration of embedded single-layer graphene sheets using equivalent nonlocal elasticity approach. *Compos Struct* 96:57–63
 92. Kitipornchai S, He XQ, Liew KM (2005) Continuum model for the vibration of multilayered graphene sheets. *Phys Rev B* 72(7):075443
 93. Nayfeh AH, Mook DT (2008) *Nonlinear oscillations*. Wiley, New York
 94. Azrar L, Benamar R, White RG (1999) Semi-analytical approach to the non-linear dynamic response problem of S–S and C–C beams at large vibration amplitudes part I: general theory and application to the single mode approach to free and forced vibration analysis. *J Sound Vib* 224(2):183–207
 95. Azrar L, Benamar R, White RG (2002) A semi-analytical approach to the non-linear dynamic response problem of beams at large vibration amplitudes, Part II: multimode approach to the steady state forced periodic response. *J Sound Vib* 255(1):1–41

Publisher's Note Springer Nature remains neutral with regard to jurisdictional claims in published maps and institutional affiliations.